

## 3D casing-distributor analysis with a novel block coupled OpenFOAM solver for hydraulic design application

C Devals<sup>1</sup>, Y Zhang<sup>1</sup>, J Dompierre<sup>1</sup>, T C Vu<sup>2</sup>, L Mangani<sup>3</sup>, F Guibault<sup>1</sup>

<sup>1</sup> École Polytechnique de Montréal, Montréal, QC, Canada

<sup>2</sup> Andritz Hydro, Pointe-Claire, QC, Canada

<sup>3</sup> Lucerne University of Applied Sciences and Arts, Technik & Architektur, Horw, Switzerland

Email: [christophe.devals@polymtl.ca](mailto:christophe.devals@polymtl.ca)

**Abstract.** Nowadays, computational fluid dynamics is commonly used by design engineers to evaluate and compare losses in hydraulic components as it is less expensive and less time consuming than model tests. For that purpose, an automatic tool for casing and distributor analysis will be presented in this paper. An in-house mesh generator and a Reynolds Averaged Navier-Stokes equation solver using the standard  $k-\omega$  SST turbulence model will be used to perform all computations. Two solvers based on the C++ OpenFOAM library will be used and compared to a commercial solver. The performance of the new fully coupled block solver developed by the University of Lucerne and Andritz will be compared to the standard 1.6ext segregated *simpleFoam* solver and to a commercial solver. In this study, relative comparisons of different geometries of casing and distributor will be performed. The present study is thus aimed at validating the block solver and the tool chain and providing design engineers with a faster and more reliable analysis tool that can be integrated into their design process.

### 1. Introduction

Nowadays, computational fluid dynamics (CFD) is commonly used by design engineers to evaluate and compare losses in hydraulic components as it is less expensive and less time consuming than model tests. In an industrial world with constantly decreasing turn-around times, engineers need automatic tools to mesh, prepare, solve and analyze their designs. In the context of hydraulic turbines, the component's global performance must be rapidly achieved. Efforts must therefore be devoted to the validation of computational schemes and to simplify the methodology used. This will allow engineers to reach adequate levels of precision in a reasonable time frame by using relatively modest computational resources.

For that purpose, an automatic tool for casing and distributor analysis will be presented in this paper. The goal of a spiral casing is to distribute the water flow as evenly as possible to the stay vanes [1]. Hydraulic turbine guide vanes control the turbine flow rate by varying their opening positions and, at the same time, provide swirling flow into the runner [2]. As mentioned in [3-4], in a good spiral casing, the pressure head of the fluid is made available to the runner with minimum loss. A few references on the casing flow simulation can be found, for instance in [1-5].

An in-house mesh generator and a Reynolds Averaged Navier-Stokes (RANS) equations solver using the standard  $k-\omega$  shear stress transport (SST) turbulence model will be used to perform all computations. Because speed and robustness are very important for CFD software, two solvers based



on the C++ OpenFOAM library [6] will be used and compared to a commercial code. The performance of the new fully coupled block solver developed by the University of Lucerne and Andritz will be compared to the standard 1.6ext segregated *simpleFoam* solver and to a commercial code.

The present study is thus aimed at validating the block solver and the tool chain and providing design engineers with a faster and more reliable analysis tool that can be integrated into their design process.

The present paper describes a methodology based on CFD to assess and validate flow field in casing and distributor components. The paper is structured as follows: first, the geometry and the mesh procedure are described in section 2 and 3 respectively. Next the proposed CFD methodology is introduced in section 4. The following section 5 presents and discusses validation of loss prediction, and the paper ends with conclusions.

## 2. Geometry

In this study, relative comparisons of two different geometries of casing adapted to one distributor will be performed. The spiral casings have a distributor height/throat diameter ratio (HDratio) of 0.35 and 24 guide vanes. For validation purpose, two guide vane opening angles will be computed: 30 and 42 degrees.

## 3. Mesh generation

An automatic meshing tool for casing and distributor analysis is presented in this section. The geometry, as shown in figure 1, was imported into Andritz design tool for casing and distributor geometry.



**Figure 1.** Casing-distributor 3D geometry

As already mentioned, the computational flow domain, as shown in figure 2, comprises the spiral casing with all the stay vanes (stv) and guide vanes (gv). Stv and gv define the distributor. The challenge in the meshing for such a geometry is the capability to automatically generate, without human intervention, casing and distributor meshes for different guide vane opening angles. In order to facilitate the meshing task, the flow domain has been divided into two sub-domains; one for the spiral casing; and the other for the distributor. In-house automatic grid generators providing hexahedral and prismatic elements are used to generate the meshes for both components. The distributor mesh has to be generated for every change in guide vane opening position while the casing mesh is generated once. In order to accommodate the meshing for different guide vane positions from closing to full opening, the distributor mesh contains concentrated hexahedral elements in the vicinity of the vane profiles to resolve the flow boundary layer and prismatic elements in the flow field. The technology on this type of hybrid mesh can be found in [7]. The spiral casing mesh contains only hexahedral elements.

The casing mesh with 2315k vertices and 2185k elements and the distributor mesh with 6500k vertices and 9900k elements were exported in the CGNS (CFD General Notation System) format [8]

and are shown in figure 2. The average first node wall distance  $Y^+$  is comprised between 9 and 23 for the *simpleFoam* (SF) solver and between 35 and 55 for the coupled solver (Coupled) and the commercial solver (CS). The minimum, average and maximum values for each operating points are given in table 1. Figures 3 and 4 show the  $Y^+$  values on the spiral casing and the distributor walls.

**Table 1.**  $Y^+$  for the different operating conditions for mesh of figure 2.

solver	casing wall			bottom ring			head cover			stay vanes			guide vanes		
	min	ave	max	min	ave	max	min	ave	max	min	ave	max	min	ave	max
SF	0.000001	8.7	75.1	0.18	20.4	36.4	0.19	20.4	36.5	0.67	12.8	27.6	3.18	22.5	32.3
Coupled	0.63	35.5	206.1	7.31	48.2	75.9	7.04	48.2	75.9	11.3	40.2	59.4	17.0	54.2	63.7
CS	0.47	35.5	179.2	3.59	48.1	74.1	3.34	48.1	74.1	5.11	38.4	56.2	9.95	55.5	65.0

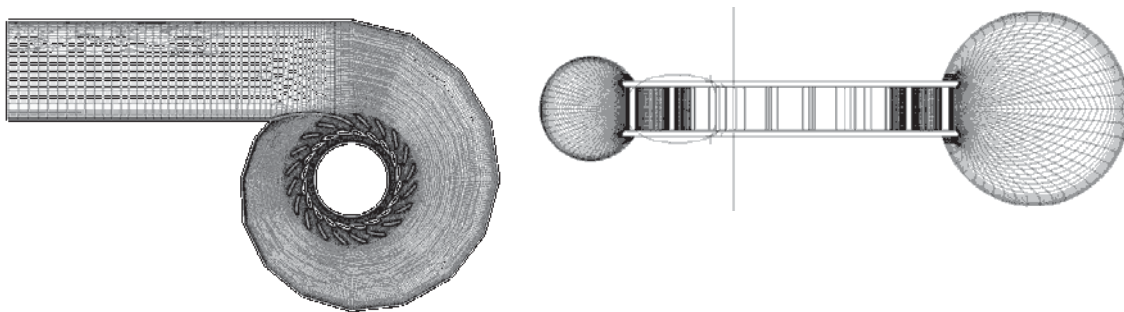


**Figure 2.** Casing-distributor mesh – Plane view  $z=0$  (left) – Section view  $y=0$  (right)

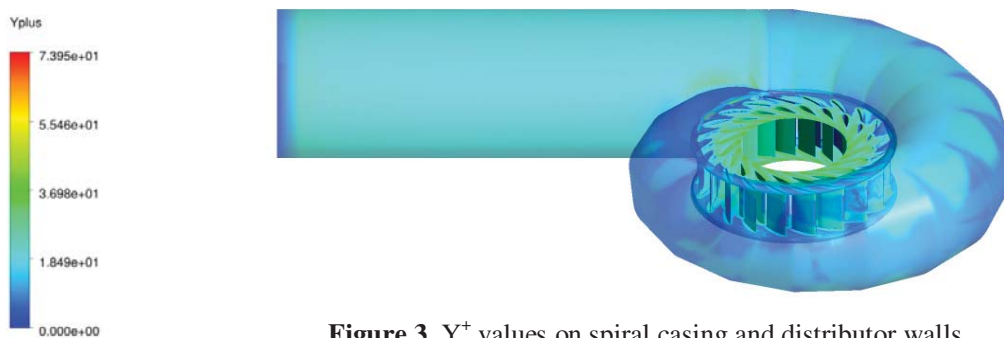


**Figure 3.**  $Y^+$  values on spiral casing and distributor walls



**Figure 4.**  $Y^+$  values on distributor walls

Once the mesh has been generated, an automatic script creates all necessary files for the OpenFOAM calculations.

#### 4. Computational Fluid Dynamics setup

The motion of fluid is described by the incompressible Navier-Stokes equations written as following:

$$\nabla \cdot \underline{u} = 0 \quad (1)$$

$$[\nabla \cdot (\underline{uu})] = -\frac{1}{\rho} \nabla p + \nabla \cdot (\nu_{eff} (\nabla \underline{u})) \quad (2)$$

##### 4.1. Segregated incompressible CFD solver: *simpleFoam*

The standard 1.6ext segregated *simpleFoam* solver based on the C++ OpenFOAM library was used for the steady state flow computations. OpenFOAM (Field Operation and Manipulation) is an open source package under GNU General Public Licence [9]. The *simpleFoam* solver is a steady-state solver for incompressible, turbulent flow of Newtonian and non-Newtonian fluids. It has been validated in [10] for the FLINDT project and in [11-12] for the Turbine-99 project. The 3D RANS equations solver using the standard k- $\omega$  SST turbulence model with wall-function are used to perform all computations [13].

*4.1.1. Numerical scheme.* An upwind convection scheme was used for all terms except  $\nabla \cdot (\underline{uu})$ . For the  $\nabla \cdot (\underline{uu})$  term (first term in the LHS of equation (2)), two schemes are used in sequence: in the first ten iterations, the upwind convection scheme is used to help convergence. Then an improved bounded normalized variable diagram (NVD) scheme GammaV was specified with a coefficient  $\psi=1.0$  after 10 iterations [14]. To solve the flow equations, the pre-conditioned bi-conjugate gradient (PBiCG) linear solver was used for all variables except pressure, for which the pre-conditioned conjugate gradient (PCG) was specified. Absolute and relative solution tolerances (tolerance and relTol) were specified for each solution variable to control the solver convergence. The tolerance is applied to the residual evaluated by substituting the current solution into the equation and taking the magnitude of the difference between the left and right hand sides [14]. relTol is the ratio of final over initial residual. In this study, a tolerance value of  $10^{-6}$  and a relTol value of 0 have been used for all variables except pressure, for which a tolerance value of  $10^{-5}$  and relTol 0.0001 were applied. A relaxation factor of 0.3 for pressure and 0.7 for other variables was also applied to improve stability. The finite volume method is applied and the coupling of the velocity and pressure equations is performed using the SIMPLE algorithm.

*4.1.2. Boundary conditions.* The inlet boundary condition is steady and mass flow average is imposed and set to  $2.358 \text{ m}^3 \cdot \text{s}^{-1}$  which give a Reynolds number based on throat diameter of  $3.3 \times 10^6$ . Two General Grid Interfaces (GGI) [15] are used in the intake and one between the spiral casing and the distributor. At the wall, no slip velocity conditions are used. At the outlet of the distributor, an average constant pressure of 0 Pa is used. The turbulence variable k,  $\epsilon$  and  $\omega$  are initialized with  $3/2(I V_{inlet})^2$ ,  $C_{mu}^{0.75} k^{1.5} / L_t$  and  $\epsilon / (C_{mu} k)$  respectively, where I is the turbulence intensity,  $V_{inlet}$  is the velocity at the inlet based on the mass flow rate,  $C_{mu}$  is the k- $\epsilon$  model parameter typically set to 0.09 and  $L_t$  is the turbulent mixing length.

*4.1.3. Additional information.* A maximum of 2000 iterations has been performed. The computations have been run in parallel on 12 CPUs on a Linux CentOS 5.5 cluster, using the Metis mesh decomposition method. Typical CPU time is less than 82961s for one operating point.

##### 4.2. Block coupled incompressible CFD solver: *coupledSteadyIncFoam*

Speed and robustness are among the most important requirements for any software that is plugged into an optimization loop. When programming a CFD code, the best way of combining both requirements is to couple the governing equations implicitly, since resolving the pressure-velocity coupling is essential for the performance of any CFD code. However up until today the SIMPLE family of algorithms [16] which couples the governing equations only by means of sub-looping, solving

sequentially each governing equation, still remains the predominant methodology used in the CFD community. Therein a segregated approach in resolving the pressure velocity coupling is followed. Compared to block coupled implicit algorithms, segregated algorithms lack scalability with mesh size robustness and calculation speed, which is inherent due in part to the under-relaxation needed to stabilize the algorithm.

In order to overcome these shortcomings, Mangani et al. [17-18] developed a block coupled incompressible solver using the open-source CFD library OpenFOAM as programming platform. Therein the algebraic equations resulting from the Navier-Stokes equations are solved simultaneously. To enhance computational performance an algebraic multi-grid solver has been implemented and used for the solution of the block-coupled system of equations.

The discretization is then cast into a block coupled linear system of equations, which is solved simultaneously.

$$\begin{bmatrix} a_C^{uu} & a_C^{uv} & a_C^{uw} & a_C^{up} \\ a_C^{vu} & a_C^{vv} & a_C^{vw} & a_C^{vp} \\ a_C^{wu} & a_C^{wv} & a_C^{ww} & a_C^{wp} \\ a_C^{pu} & a_C^{pv} & a_C^{pw} & a_C^{pp} \end{bmatrix} \begin{bmatrix} u_C \\ v_C \\ w_C \\ p_C \end{bmatrix} + \sum_{NB} \begin{bmatrix} a_{NB}^{uu} & a_{NB}^{uv} & a_{NB}^{uw} & a_{NB}^{up} \\ a_{NB}^{vu} & a_{NB}^{vv} & a_{NB}^{vw} & a_{NB}^{vp} \\ a_{NB}^{wu} & a_{NB}^{wv} & a_{NB}^{ww} & a_{NB}^{wp} \\ a_{NB}^{pu} & a_{NB}^{pv} & a_{NB}^{pw} & a_{NB}^{pp} \end{bmatrix} \begin{bmatrix} u_{NB} \\ v_{NB} \\ w_{NB} \\ p_{NB} \end{bmatrix} = \begin{bmatrix} b_C^u(u, v, w, p) \\ b_C^v(u, v, w, p) \\ b_C^w(u, v, w, p) \\ b_C^p(u, v, w, p) \end{bmatrix} \quad (3)$$

Segregated algorithms, as *simpleFoam*, operate using many sub-loops to account for inter-equation coupling, continuously updating the RHS of (4), which contains field values of previous iteration steps.

$$\begin{aligned} a_C^u \cdot u_C + \sum_{NB} a_{NB}^u \cdot u_{NB} &= b_C^u(u, v, w, p) \\ a_C^v \cdot v_C + \sum_{NB} a_{NB}^v \cdot v_{NB} &= b_C^v(u, v, w, p) \\ a_C^w \cdot w_C + \sum_{NB} a_{NB}^w \cdot w_{NB} &= b_C^w(u, v, w, p) \\ a_C^p \cdot p_C + \sum_{NB} a_{NB}^p \cdot p_{NB} &= b_C^p(u, v, w, p) \end{aligned} \quad (4)$$

Additionally, under-relaxation of the governing equations is needed to ensure that the solution process remains numerically stable. In block coupled algorithms, sub-looping is also applied in order to update second order derivative terms and non-linear terms. However, in contrast to segregated algorithms, the inter-variable coupling is still much stronger and fewer sub-loops are needed. Also under-relaxation can be completely avoided using so-called false transient time stepping. The solution of its discretized system of equations therefore turns out to be numerically much more stable than that of segregated algorithms and also significantly faster in terms of calculation time, which has been demonstrated by Mangani et al. [17-18]. Therein, a  $k-\omega$  SST turbulence model has been solved in addition to momentum and continuity equations.

**4.2.1. Numerical Schemes:** All the simulations were performed with a fully second order upwind discretization. Special schemes were developed in order to keep the stability and robustness also for the accelerated algorithm. Moreover no special switching to first order was necessary at the beginning of the simulations as contrary that was needed for the standard *simpleFoam* solver.

**4.2.2. Boundary conditions:** The inlet boundary condition is steady and mass flow average is imposed and set to  $2.358 \text{ m}^3\text{s}^{-1}$ . Two GGI interfaces are used in the intake and one between the spiral casing

and the distributor. At the wall, no slip velocity conditions are used. At the outlet of the distributor, an average constant pressure of 0 Pa is used. The turbulence variables  $k$ ,  $\epsilon$  and  $\omega$  are initialized as in section 3.1.2.

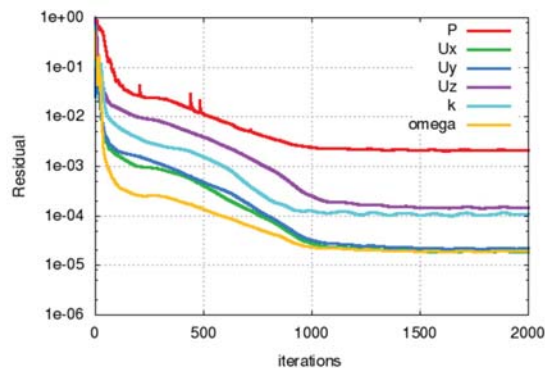
#### 4.3. Commercial solver (CS)

**4.3.1. Numerical scheme.** A commercial software implementing the standard RANS model using a two-equation  $k$ - $\omega$  SST turbulence closure model was used to perform all computations. The commercial solver is a code based on the finite volume method which implements several discretization schemes. All computations were performed using an automatic numerical stability based blended first and second order scheme for the momentum equations, and the first order upwind scheme for the turbulent advection equations. For steady state computations, the convergence criterion was set to  $5 \times 10^{-6}$  on the root mean square (RMS) residuals for all primitive variables. We have imposed a minimum of 100 iterations and a maximum of 500 iterations for all computations. The pseudo time step option for steady state cases was set to auto timescale which gives a value of 0.268s and the timescale factor was set to 1.0.

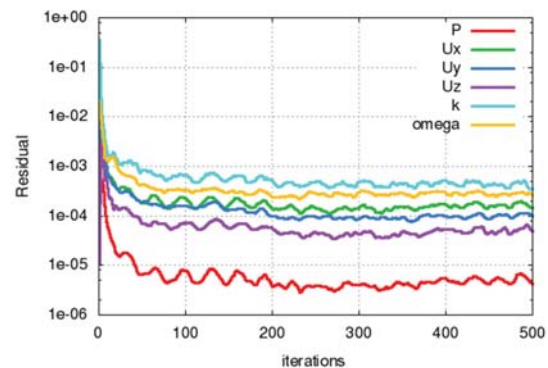
**4.3.2. Boundary conditions.** The same types of boundary conditions than the other solvers have been imposed: mass flow at the inlet, GGI interfaces, non-slip wall velocity, average constant pressure at the outlet.

### 5. Results and discussion

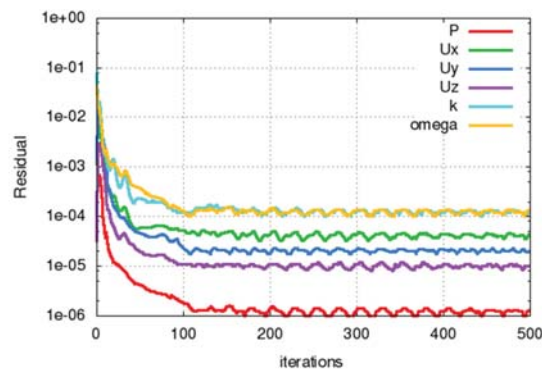
Figures 5, 6 and 7 show typical converged graphs. The *simpleFoam* residuals are computed in a different way than for the two other codes, therefore making it difficult to fix only one residual target. For the *simpleFoam* solver, convergence is reached in approximately 1200 iterations (figure 5), compared to the coupled solver with 60 iterations (figure 6) and the commercial solver with 120 iterations (figure 7) based on average monitor points and integral quantities.



**Figure 5.** Geometry 1 - guide vane opening angle of 30 degrees – *SimpleFoam*



**Figure 6.** Geometry 1 - guide vane opening angle of 30 degrees - Coupled solver



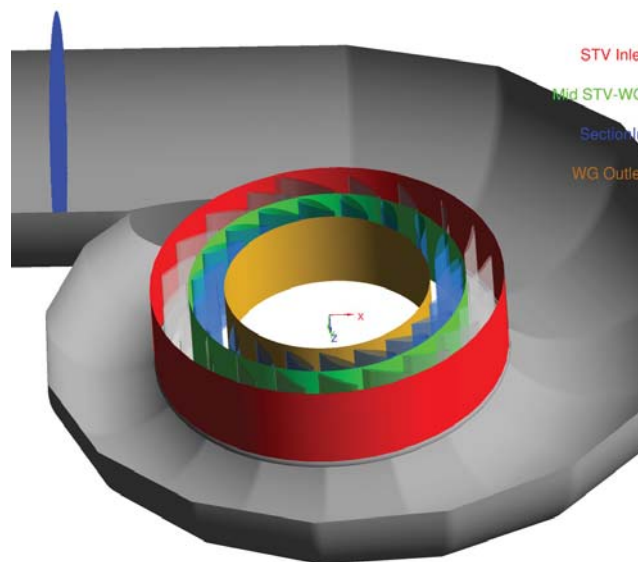
**Figure 7.** Geometry 1 - guide vane opening angle of 30 degrees - Commercial solver

Table 2 shows that the coupled solver is much faster compared to the *simpleFoam* solver and relatively fast compared to the commercial solver even if the time per iteration is higher, because the converged solution is reached very rapidly.

**Table 2.** Speed up factor

	SF	Coupled	CS
Time per iterations (s)	465.66	623.93	420.39
Converged solution	1200	60	120
Speed up factor	1	15	11

Figure 8 shows all the planes used for component losses: entrance of the casing in blue (referred as SectionIn in table 3), stv inlet in red, mid stv-wg in green and wg outlet in brown.



**Figure 8.** Planes for loss calculations

Table 3 shows the total pressure on extracted planes shown in figure 8. The total pressure computed by the coupled solver and the commercial solver are very similar (less than 0.4%). For the *simpleFoam* solver, the difference is lower by about 2% compared to the two other codes.

**Table 3.** Total pressure (in Pa) on planes shown in figure 8 for Geometry 1

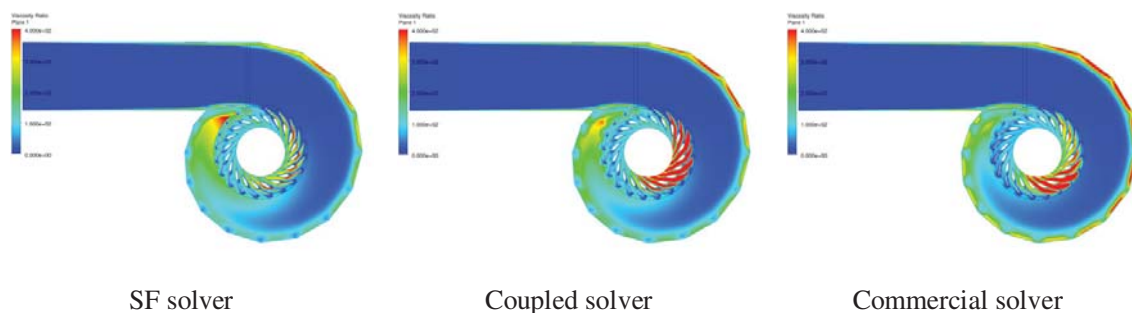
		SF	Coupled	CS
GV30	SectionIn	12666.33	12963.90	12983.37
	Stv Inlet	12611.84	12895.00	12922.27
	Mid Stv-Wg	12451.21	12725.86	12763.69
	Wg Outlet	12173.06	12427.89	12479.15
GV42	SectionIn	6568.465	6721.1929	6705.913
	Stv Inlet	6512.882	6653.2798	6644.679
	Mid Stv-Wg	6353.435	6482.9746	6494.450
	Wg Outlet	6204.168	6319.5444	6336.661

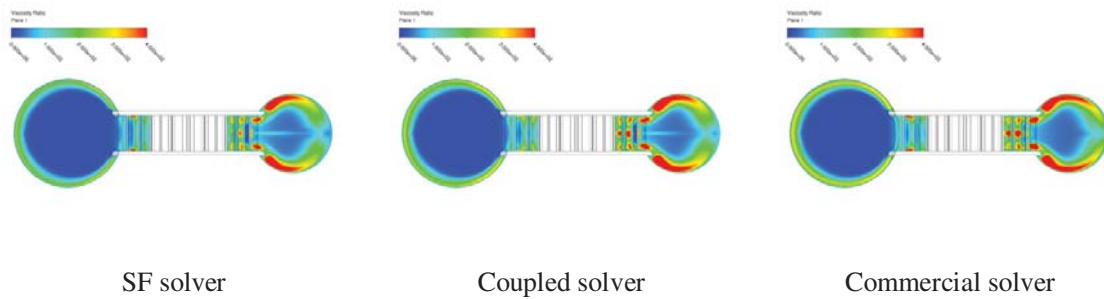
The losses are defined as  $(ptotPlaneIn - ptotPlaneOut) * 100 * C / (0.5 * \rho * V_{Dth}^2)$ , where  $V_{Dth}$  is the velocity at the throat diameter, C is a constant, ptotPlaneIn and ptotPlaneOut are one of the four planes SectionIn, Stv Inlet, Mid Stv Wg and Wg Outlet. These component losses are shown in table 4. The losses of the coupled solver are higher compared to the two other codes, however the tendencies are identical. The total losses of Geometry 1 are smaller than Geometry 2 because Geometry 1 is larger than Geometry 2.

**Table 4.** Component losses [% $\rho gH$ ] for  $Q_{11}=1 \sqrt{m/s}$ .

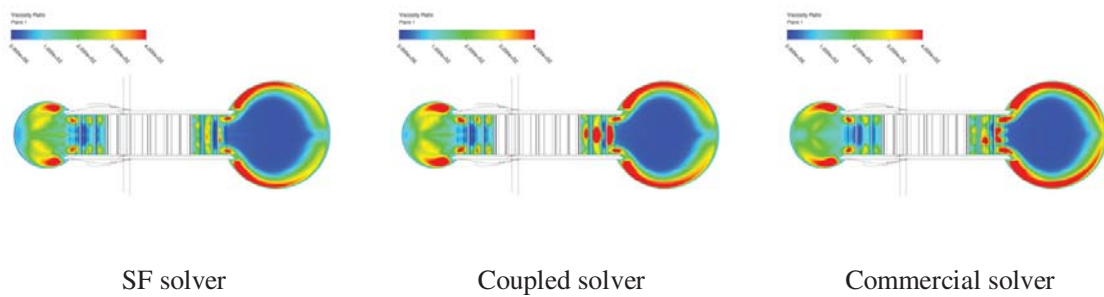
		SF		Coupled		CS	
		Casing	Distributor	Casing	Distributor	Casing	Distributor
Geometry 1	GV30	0.1002	0.8068	0.1267	0.8588	0.1123	0.8146
	GV42	0.1022	0.5676	0.1249	0.6136	0.1126	0.5662
Geometry 2	GV30	0.1338	0.8131	0.1509	0.8679	0.1418	0.8373
	GV42	0.1346	0.5697	0.158	0.6147	0.1421	0.5861

Figures 9, 10 and 11 show the viscosity ratio in plane xy, yz and zx respectively. Similar results are obtained in all figures. In figure 9, SF solver produces more viscosity at the end of the casing, but less in the middle of the stay vanes and guide vanes compared to the two other codes. Similar trends are also visible in figure 10 and 11.

**Figure 9.** Viscosity ratio on xy plane



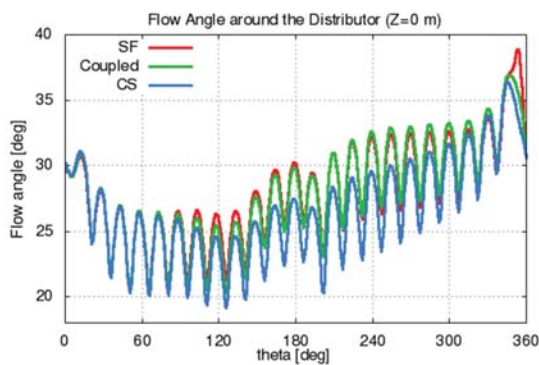
**Figure 10.** Viscosity ratio on yz plane



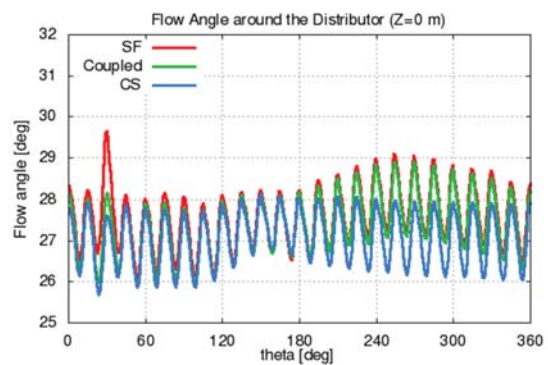
**Figure 11.** Viscosity ratio on zx plane

Figure 12 shows the flow angle upstream stay vane leading edges and figure 13 the flow angle downstream guide vane trailing edges for the three different solvers. The zero theta starts at the baffle position. Some differences are visible: for the *simpleFoam* solver, the flow angle at 360 is slightly higher than the two other codes and for the commercial solver the flow angle is smaller between 90 and 330 degrees.

In the same manner, figures 14 and 15 show the radial velocity upstream stay vane leading edges and downstream guide vane trailing edges for the three different solvers. Similar comments are made.



**Figure 12.** Flow angle upstream of stay vane leading edges



**Figure 13.** Flow angle downstream guide vane trailing edges

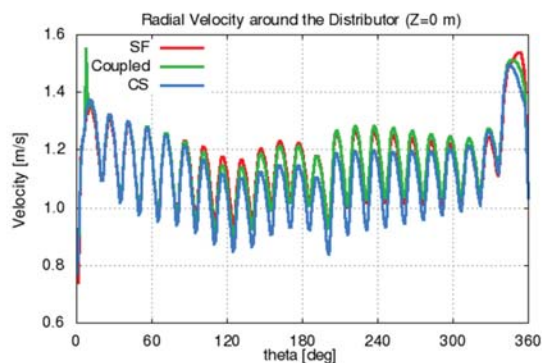


**Figure 14.** Radial velocity upstream of stay vane leading edges

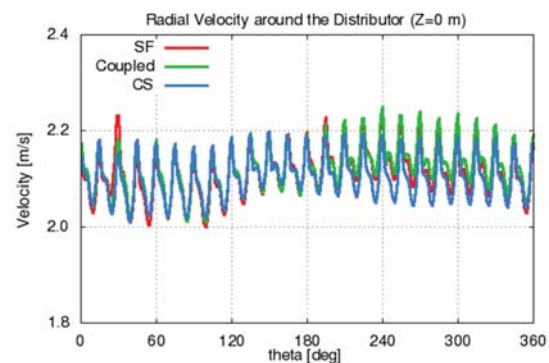


**Figure 15.** Radial velocity downstream guide vane trailing edges

## 6. Conclusion

Simulations of a full 3D casing-distributor have been performed with three different solvers. It appears that the new OpenFOAM coupled solver is very fast and gives similar results compared to the two other codes. Robustness and speed are qualities that are required for CFD codes, especially if it is plugged in a CFD tool chain for optimization or design purpose, and the new OpenFOAM coupled solver meets this requirement.

Of course, these validations were only preliminary results and a deep validation work must be pursued on other geometries.

## References

- [1] Geberkiden BM and Cervantes M 2007 Effects on inlet boundary conditions on spiral casing simulation 2<sup>nd</sup> IAHR International Meeting of the Workgroup on Cavitation and Dynamic Problems in Hydraulic Machinery and Systems (October 24-26, 2007. Timisoara, Romania)
- [2] Vu TC, Devals C, Disciullo J, Iepan H, Zhang Y, and Guibault F 2012 CFD methodology for desynchronized guide vane torque prediction and validation with experimental data. 26<sup>th</sup> IAHR Symposium on Hydraulic Machinery and Systems (August 19-23, 2012. Beijing, China)
- [3] Biswas G et al 1998 A numerical study on flow through the spiral casing of a hydraulic turbine. *International Journal for Numerical Methods in Fluids* **28**(1) 143-156
- [4] Maji PK and Biswas G 2000 Analysis of flow in the plate-spiral of a reaction turbine using a streamline upwind Petrov–Galerkin method. *International Journal for Numerical Methods in Fluids* **34**(2) 113-144
- [5] Oliveira de Souza LCE et al 2003 Assessment of turbulence modelling for CFD simulations into hydroturbines: spiral casings 17<sup>th</sup> International Mechanical Engineering Congress (São Paulo, Brazil)
- [6] OpenFOAM web site. Available at <http://www.openfoam.com/>
- [7] Guibault F, Zhang Y, Dompierre J and Vu TC 2006 Robust and Automatic CAD-based Structured Mesh Generation for Hydraulic Turbine Component Optimization 23<sup>rd</sup> IAHR Symposium on Hydraulic Machinery and Systems (October 17-21, 2006. Yokohama, Japan)
- [8] Allmaras, S. and McCarthy D. CGNS CFD Standard Interface Data Structures - Version 3.2.1. CGNS Project Group 2004 Available at: [http://www.grc.nasa.gov/WWW/cgns/CGNS\\_docs\\_current/sids](http://www.grc.nasa.gov/WWW/cgns/CGNS_docs_current/sids)
- [9] GNU web site. Available at <http://www.gnu.org/>
- [10] Vu TC, Devals C, Zhang Y, Nennemann B and Guibault F 2011 Steady and unsteady flow computation in an elbow draft tube with experimental validation *Int. J. Fluid Machinery and*

- Systems* **4**(1) 85-96
- [11] Tanase NO, Bunea F and Ciocan GD 2012 Numerical simulation of the Flow in the Draft Tube of the Kaplan Turbine *UPB Sci. Bull., Series D* **74**(1)
  - [12] Nilsson H 2006 Evaluation of OpenFOAM for CFD of turbulent flow in water turbines *23rd IAHR Symposium on Hydraulic Machinery and Systems* (October 17-21, 2006. Yokohama, Japan)
  - [13] Menter FR 1994 Two-Equation Eddy-Viscosity Turbulence Models for Engineering Applications *AIAA Journal* **32**(8)
  - [14] OpenFOAM User Guide. Available at <http://www.openfoam.org/docs/user/>
  - [15] Beaudoin M and Jasak H 2008 Development of a Generalized Grid Interface for Turbomachinery simulations with OpenFOAM *OpenSource CFD International Conference*, (December 4-5, 2008. Berlin, Germany)
  - [16] Patankar S and Spalding D 1972 A calculation procedure for heat, mass and momentum transfer in three-dimensional parabolic flows *International Journal of Heat and Mass Transfer* **15**
  - [17] Mangani L, Buchmayr M and Darwish M 2013 Development of a Novel Fully Coupled Solver in OpenFOAM: Steady State Incompressible Turbulent Flows *accepted by Numerical Heat Transfer Part B: Fundamentals*
  - [18] Mangani L, Buchmayr M and Darwish M 2013 Development of a Novel Fully Coupled Solver in OpenFOAM: Steady State Incompressible Turbulent Flows in Rotational Reference Frames *accepted by Numerical Heat Transfer Part B: Fundamentals*